Available online at www.sciencedirect.com
SCIENCE DIRECT®
Vacuum 79 (2005) 100–105
VACUUM
SURFACE ENGINEERING, SURFACE INSTRUMENTATION & VACUUM TECHNOLOGY
www.elsevier.com/locate/vacuum

Fabrication of nano-scale optical patterns in amorphous silicon carbide with focused ion beam writing ☆

T. Tsvetkova[a,*], S. Takahashi[b], A. Zayats[b], P. Dawson[b], R. Turner[b], L. Bischoff[c], O. Angelov[d], D. Dimova-Malinovska[d]

[a]*Bulgarian Academy of Science, Institute of Solid State Physics, 72 Tzarigradsko Chaussee, 1784 Sofia, Bulgaria*
[b]*School of Mathematics and Physics, The Queen's University of Belfast, Belfast BT7 1NN, UK*
[c]*Forschungszentrum Rossendorf e. V., P.O. Box 510119, D-01314 Dresden, Germany*
[d]*Central Laboratory for Solar Energy, 72 Tzarigradsko Chaussee, 1784 Sofia, Bulgaria*

Received 14 June 2004; received in revised form 3 February 2005; accepted 4 February 2005

Abstract

Optical patterns as small as 200 nm width have been fabricated in a thin film of amorphous silicon carbide (a–SiC:H) using a focused ion beam microscope, (FIB). Because of the low electric conductivity of a–SiC:H, the diameter of the writing ion beam is broadened by the effect of surface charging which was overcome by depositing a thin layer of gold onto the a–SiC:H film. The topographic and optical contrasts of the patterned thin films have been mapped with scanning near-field optical microscopy. The optical contrast corresponding to nanostructures is 0.2 with an overall increase of the optical density contrast of 0.5 in the irradiated areas. The results of the fabrication of patterns created with FIB on aluminium-coated a-SiC:H films are also briefly presented.

Keywords: Amorphous silicon carbide (a–SiC:H); Focused ion beams; Scanning near-field optical microscopy (SNOM); Nano-scale optical data storage

1. Introduction

Hydrogenated amorphous silicon carbide (a–SiC:H) alloy films have great technological potential as structural materials for high-temperature electronics and for various optoelectronic elements and devices designed to operate in aggressive environments (acid vapours, radiation, open space, etc.) [1,2]. An important feature

☆ Paper originally presented at ION 2004, the V-th International Conference Ion Implantation and Other Applications of Ions and Electrons, Kazimierz-Dolny, Poland, 2004.

*Corresponding author. Tel.: +359 271 446 58; fax: +359 297 536 32.
E-mail address: tsvet@issp.bas.bg (T. Tsvetkova).

0042-207X/$ - see front matter © 2005 Elsevier Ltd. All rights reserved.
doi:10.1016/j.vacuum.2005.02.001

underpinning the material's environmental robustness is the comparatively wide band gap which may be tailored in the range 1.8–3.0 eV.

The material can be prepared in thin film form on different substrates by chemical vapour deposition [3], or by employing a radio-frequency reactive magnetron sputtering method [4]. Mechanical, optical and electrical parameters of the material can be controllably varied by changing the relative composition of the constituent elements. In addition, control of electronic and optical properties of such materials can be achieved using ion implantation [5,6]. Recently, using the emerging technology of ion micro-beams [9], promising results have been obtained for the possible application of thin silicon carbide films in high-density optical data storage and sub-micron lithography [7,8]. This approach has been further developed, by implementing ion doping with focused ion beam (FIB) systems that use Ga^+ or other chemically active ion species as implants [10–13].

The fabrication of nano-scale patterns on a–SiC:H films with focused ion beams is not straightforward. Due to the low electric conductivity of silicon carbide, the surface is easily charged by the ion-beam irradiation, leading to the defocusing of the ion beam. Therefore, the first experiments using FIB-based implantation have been restricted to micron-scale patterning [8,12]. One of the techniques to avoid charging of the sample surface is to employ a charge neutralizer, where an electron beam is used for irradiation of the surface simultaneously with the Ga^+ ion beam thus cancelling the net electric charge on the sample surface. Another technique to avoid the charge-up problem is to deposit a conductive layer, such as metal or carbon, on the substrate surface. This technique is well established and routinely employed in the field of electron microscopy analysis, and thus suggests its possible application for surface milling. However, after patterning, such a metallic layer should be removed, and it is yet to be verified how the removal of coating affects the sharpness of the optical patterns. In addition, since removal of the metallic coating decreases the transmission of the sample while ion implantation into the a–SiC:H layer increases the optical density of the film, both effects may cancel one another. Thus, it is necessary to investigate which effect is dominant after ion irradiation.

In the present work, Au-coated a–SiC:H films were used to fabricate nano scale patterns using the FIB technique. The patterns obtained were first mapped with Atomic Force Microscopy (AFM) [14,15] to investigate topographic profiles. In addition, near-field optical microscopy (SNOM) [15–17] was used to acquire optical profiles of the samples. Finally the nano-patterning on Al-coated a–SiC:H is briefly discussed.

2. Experimental

Thin a–$Si_{1-x}C_x$:H films ($x = 0.15$) were deposited onto Corning glass substrates by RF (13.56 MHz) reactive magnetron sputtering. A composite target, composed of mono-crystalline (1 0 0) silicon wafer with chips of pure graphite placed on it, was sputtered in an Ar-20% H_2 gas mixture. Typical deposition conditions are RF power 150 W (power density 1.91 W/cm^2), total gas pressure 1P, substrate temperature 275 °C, and graphite-to-silicon target ratio 0.025. The film thickness was determined by Talystep profilometry and conventional far-field optical absorption measurements to be ~200 nm. Rutherford backscattering spectrometry was used to determine the carbon content, x, of the films.

Focused Ga^+-ion beam implantation of the samples was performed by a computer-controlled FIB system (model FEI-FIB200-TEM) to produce various preliminary designed optical patterns. The a–SiC:H films were over-coated with a thin metal layer of Au or Al. The thickness of the metal layer was about 10 nm. The metallic coating was grounded in order to avoid build-up of electric charge on the film surface during processing with the focused Ga^+ ion beam.

An AFM (model Dimension 3000, Digital Instruments) was used to analyse the topography of the various implanted patterns. A lab-built SNOM was used to map the optical absorption of the patterned areas with sub-wavelength resolution and thus achieve a relevant measure of the

optical contrast between the ion irradiated and non-irradiated regions of the sample [18].

3. Results and discussion

In order to check the topographic features of the patterns, AFM images of three different patterns are recorded. The results are presented in Figs. 1–3. These patterns comprise of: a full square ($2 \times 2\,\mu m$, Fig. 1), an open square ($2 \times 2\,\mu m$, Fig. 2) formed with lines of 100 nm depth and width, and a series of lines with length/width/depth 2.0/0.1/0.1 μm (Fig. 3). Each figure presents a two-dimensional image and a typical cross section. The depth of the topographic features is as large as 100 nm, which is ten times larger than the thickness of the Au-coating (10 nm). This confirms that the ion beam reaches the a–SiC:H layer and that ion-implantation should occur.

An important feature of these images is that the edge and line resolution is of the order of 100–150 nm, which is sharper than the line widths obtained for the combination of charge neutralizer and bare a–SiC:H surfaces[18], and thus it can be concluded that by depositing a gold film, nano-scale patterning in a-SiC:H has been successfully demonstrated. In addition to the confirmation of nano-scale patterning, we can discuss the efficiency of electric grounding by comparing the edge sharpness between different patterns from the cross sections of Figs. 1–3. For the filled square (Fig. 1) and the open square (Fig. 2) the half-width at half-minimum (HWHM) of the ion-irradiated

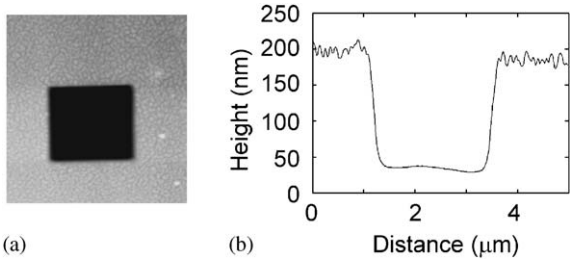

Fig. 1. Topographic image (a) and cross-sectional view (b) of a full-square pattern ($2 \times 2\,\mu m$) in the Au-coated a–SiC:H thin film, fabricated with FIB system using focused Ga^+ ion beam.

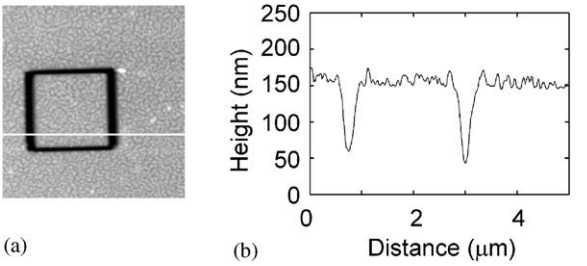

Fig. 2. Topographic image (a) and cross-sectional view (b) for an open-square pattern ($2 \times 2\,\mu m$) in the Au-coated a–SiC:H thin film, fabricated with FIB system using focused Ga^+ ion beam.

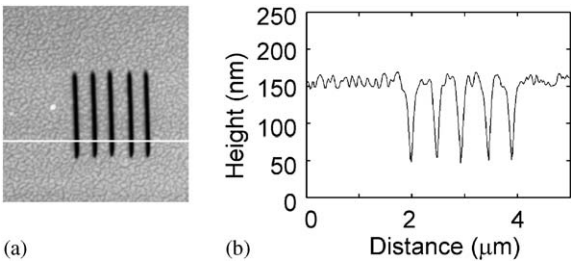

Fig. 3. Topographic image (a) and cross-sectional view (b) for a series of lines (line separation, thickness and depth are 2.0, 0.1 and 0.1 μm, respectively) in the Au-coated a–SiC:H thin film, fabricated with FIB system using focused Ga^+ ion beam.

lines is ~80 nm while for the series of lines (Fig. 3), this value is reduced to ~50 nm. It is intriguing that the HWHM of the filled square, with a large nonconductive area exposed, is equal to that of open square, in which exposed nonconductive area is a closed curve (edges of the square). This can be explained in terms of the electric connection of each part of the metallic surface to the ground. In the open square (Fig. 2), the metallic surface inside the edges of the square is electrically isolated from the outer region of the metallic film, leading to the accumulation of electric charge. Thus it can be plausible that the amount of the accumulated charge inside the open square may be as large as that for the filled square. In contrast, for a series of lines, the metallic surface is completely connected to the ground, and thus the efficiency of draining electric charge is optimized, resulting in the smaller HWHM (edge sharpness) of the lines. This result provides us with useful information with respect to

the design of more complicated patterns. Namely, each part of the metallic layer on the surface after pattern-milling should be electrically connected to ground, or at least, the milling process should be so scheduled that electrical connection of the metallic surface should be as well maintained as possible while each line is milled.

Fig. 4 presents a topographic image and corresponding near-field optical image of a set of gratings fabricated on the surface of Au-covered a–SiC:H film. The width of the lines is 100 nm and the separation between adjacent lines is 300 nm. Both images are simultaneously recorded with the SNOM. In the topographic image the grating is well resolved, while in the corresponding optical image an overall increase of absorption (dark region) is observed with fine structures corresponding to the nanostructure. Since the whole area of the surface is initially covered with a gold layer (partially) blocking the transmission of light, the transmission of light in the ion-bombarded region might be expected to be higher due to the removal of gold layer. Thus the effect of ion-implantation that results in the increase in optical density may be cancelled by the decrease in optical density owing to the ablation of the metallic coating.

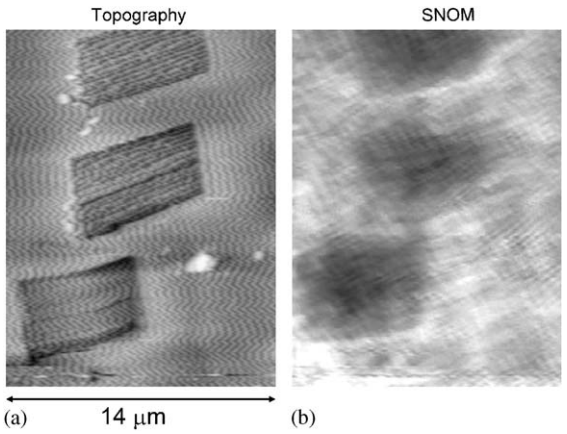

Fig. 4. Topographic image (a) and corresponding SNOM image (b) of a set of gratings created on the a–SiC:H film pre-coated with a gold layer. The width of the lines of the gratings is 100 nm and the separation between adjacent lines is 300 nm.

The optical contrast shown in Fig. 4 clearly illustrates that the effect of ion-implantation is dominant compared with that of the removal of gold. Such experimental results may help to determine the optimum thickness of the metallic coating and irradiation parameters of FIB process.

A cross section of the SNOM image was used to examine the fine structure of the optical contrast (Fig. 5). The grating in the left bottom corner of Fig. 4 is shown in Fig. 5. It is seen, as in two-dimensional mapping of the optical contrast, that the fine structure is coupled to the overall decrease of the transmission in the irradiated region. The contrast of the overall decrease in transmission, which is defined as the contrast between the average transmission in the irradiated area and that of the un-irradiated one, is about 0.5. While the contrast for the fine structure, which is determined here as the top and bottom of the modulation of transmission intensity, is about 0.2. It should be noted that the undulation of the transmission associated with the nano-scale pattern is only 10% of the overall change of transmission, but this modulation is sufficiently pronounced in optical density as long as the background (overall decrease) is flat. Near the end of the patterned area, the change of the background is large compared with the optical density modulation due to the nano-structure. Therefore, the modulation due to the nano-structure is better observed at the centre of the grating. In order to evaluate the width of the optical pattern, the full widths at half-maximum (FWHM) of the dips have been measured related to the decrease of transmission in the ion-implanted area. Some of the FWHM are as small

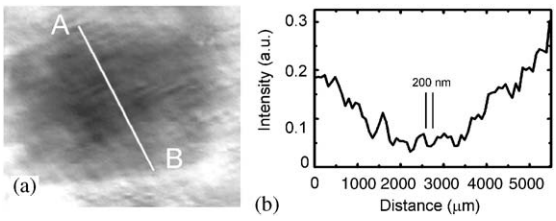

Fig. 5. A cross-sectional analysis of the SNOM image. The SNOM image shown in (a) corresponds to the grating located in the left-hand bottom of the SNOM image shown in Fig. 4. The cross-section (b) was taken along the line AB drawn in (a).

as 200 nm with a periodicity of 400 nm that is equal to the value estimated from the design of the grating (100 nm in width and 300 nm in separation). This result demonstrates the formation of nanometer-scale optical contrasts, although the line width is twice as designed. There can be two possible mechanisms that can explain these observations: (i) convolution of fine and broad variation of the optical contrasts and (ii) a larger line width than is expected by the design. One possible mechanism is that the uncoated optical fibre probe picks up background signal transmitted through the sample. It is known that SNOM images recorded with an uncoated fibre probe in transmission configuration often show such background resulting from the core diameter being larger than the size of the very end of the tip. In such cases, SNOM images show a convolution of real nanoscopic effects and the far field contributions from larger and deeper regions of the sample. The other possibility is the unfavourable modification of non-irradiated areas. This mechanism can be further categorized into two mechanisms. The first one is beam-broadening due to charge build-up in the milled region of the surface, because the sample surface becomes insulating after removal of the gold layer. Although the milled region is surrounded by a gold mask, the insulating part of the surface can still be charged up weakly. This causes an increase of the ion-beam diameter at the surface or unfavourable deflection of the beam, thus leading to irradiating of a larger area of the sample surface. The second mechanism is that of sputtering of SiC clusters around the edge of the trenches of the grating. The FIB process, as shown in topographic images, also causes the milling of the surface material in addition to the implantation of ions. It can happen that a part of surface material with higher optical absorption is sputtered away and scattered around the pattern, especially around the edges of the surface.

Finally, preliminary results of the experiments on nano-scale patterning with FIB by using Al-covered a–SiC:H samples are demonstrated. The secondary ion images recorded immediately after the FIB-milling in the vacuum chamber are shown in Fig. 6. Each pattern consists of a set of lines with 100 nm width separated differently. The secondary ion images show that a line thickness as small as 100 nm has been realized. SNOM measurements on these samples are now underway.

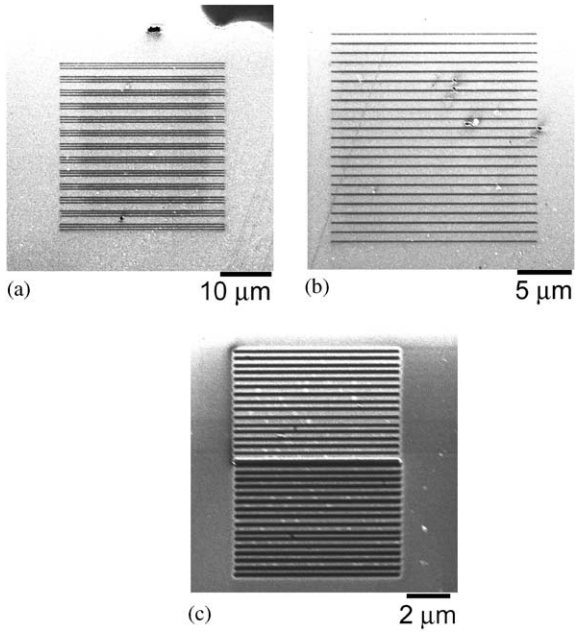

Fig. 6. Secondary ion image of (a) the triplet lines pattern (100 nm width, 300 nm separation between adjacent lines in each triplet and 1000 nm separation between triplets), (b) the low-density set of single lines (100 nm width and 900 nm separation) and (c) the high-density set of single lines (100 nm width and 300 nm separation) in an Al-coated a–SiC:H thin film, written with FIB system using focused Ga^+ ion beam.

4. Conclusion

By coating thin gold layers on thin films of a–SiC:H, nano-scale patterning using FIB irradiation has been successfully demonstrated, and an optical line width as small as 200 nm in FWHM has been observed with SNOM. According to the variations in transmission intensity associated with the nanostructures, the resultant optical contrast is about 0.2, although the absolute value of these variations are 10% of the overall decrease in transmission in the ion-implanted area. Using AFM data, we have also investigated the correlation

between the sharpness of the edge of the pattern and its geometrical shape, and have determined the importance of the integrity of electrical connections to the metallic surface for creating finer structures. Finally, we have briefly suggested the possibility of using a different kind of metal, such as Al, for obtaining more densely packed structures. The present results open up the possibility of a new application of a–SiC:H to the medium for high-density optical data storage. At present stage, topographic modification associated with ion-irradiation and the convolution of overall and finer variations in optical density are important problems to solve. It is now necessary to optimize the experimental conditions including the thickness of the metallic coating, the kind of metal to be coated, irradiation parameters such as acceleration voltage, ion current and milling time. It is believed that such optimization will allow topographically flat and optically sharp nanostructures to be obtained.

Acknowledgements

TT acknowledges the support from the International Research Centre for Experimental Physics (IRCEP), The Queen's University of Belfast, UK, where the greater part of the work was carried out. Part of the work was also performed within a joint collaboration project in the frame of the contract for scientific cooperation between the Bulgarian Academy of Sciences and FZ Rossendorf, Germany.

References

[1] Powell JA, Matus L. In: Harris GL, Yang CYW, editors. Amorphous and crystalline silicon carbide. Berlin: Springer; 1989.
[2] Kanicki J, editor. Amorphous and microcrystalline semiconductor devices. Boston, London: Artech House; 1991.
[3] Heinrich J, Hemeltjen S, Marx G. Microchim Acta 2000;133:209.
[4] Bullot J, Schmidt MP. Phys Status Solidi B 1987;143:345.
[5] Hirvonen JK. Ion implantation and ion beam processing of materials. Amsterdam: North Holland; 1984.
[6] Ziegler JF. Ion implantation. New York: Academic Press; 1988.
[7] Ruttensperger B, Krötz G, Müller G, Derst G, Kalbitzer S. J Non-Cryst Solids 1991;137-138:635.
[8] Müller G. Nucl Instrum Methods B 1993;80–81:957.
[9] Böhringer K, Jousten K, Kalbitzer S. Nucl Instrum Methods B 1988;30:289.
[10] Tsvetkova T. In: Singh J, Copley S, Mazumder J, editors. Beam processing of advanced materials. Metals Park: ASM International; 1996. p. 207.
[11] Tsvetkova T, Tzenov N, Tzolov M, Dimova-Malinovska D, Adriaenssens GJ, Pattyn H. Vacuum 2001;63:749.
[12] Bischoff L, Teichert J, Kitova S, Tsvetkova T. Vacuum 2003;69:73.
[13] Tsvetkova T, Angelov O, Sendova-Vassileva M, Dimova-Malinovska D, Bischoff L, Adriaenssens GJ, Grudzinski W, Zuk J. Vacuum 2003;70:467.
[14] Binnig G, Quate CF, Gerber Ch. Phys Rev Lett 1986;56:930.
[15] Friedbacher G, Fuchs H. Pure Appl Chem 1999;71:1337.
[16] Betzig E, Trautman JK. Science 1992;257:189.
[17] Pohl DW, Courjon D, editors. Near field optics. Kluwer Academic Publishers: Dordrecht; 1993.
[18] Tsvetkova T, Takahashi S, Zayats AV, Dawson P, Turner R, Bischoff L, Angelov O, Dimova-Malinovska D. Vacuum, to be published, doi:10.1016/j.vacuum.2005.02.002.